Gaussian mixture model for extreme wind turbulence estimation

Xiaodong Zhang, Anand Natarajan

Technical University of Denmark, Department of Wind Energy, Frederiksborgvej 399, 4000 Roskilde, Denmark

Correspondence: Xiaodong Zhang (xiazang@dtu.dk)

Abstract. Uncertainty quantification is necessary in wind turbine design due to the random nature of the environmental inputs, through which the uncertainty of structural loads and response under specific situations can be quantified. Specifically, wind turbulence (described by standard deviation of the longitudinal wind speed over a 10-minute time duration) has a significant impact on the extreme and fatigue design envelope of the wind turbine. The wind parameters (mean and standard deviation of longitudinal wind speed over 10-min time duration) are not independent stochastic variables, and therefore structural reliability analysis or uncertainty quantification requires these wind parameters to be correlated stochastic parameters. An accurate probabilistic model should be established to model the correlation among wind parameters. Compared to univariate distributions, theoretical multivariate distributions are limited and not flexible enough to model the wind parameters from different sites or direction sectors. Copula-based models are used often for correlation description, but existing parametric copulas may not model the correlation among wind parameters well due to limitations of the copula structures. The Gaussian mixture model is widely applied for density estimation and clustering in many domains, but limited studies were conducted in wind energy and few used it for density estimation of wind parameters. In this paper, the Gaussian mixture model is used to model the joint distribution of mean and standard deviation of longitudinal wind speed over 10-min time duration, which is calculated from 15 years of wind measurement time series data. As a comparison, the Nataf transformation (Gaussian copula) and Gumbel copula are compared with the Gaussian mixture model in terms of the estimated marginal distributions and conditional distributions. The Gaussian mixture model is then adopted to estimate the extreme wind turbulence (wind parameters for extreme load), which could be taken as an input to design loads used in the ultimate design limit state of turbine structures. The wind parameter contour associated with a 50-year return period computed from the Gaussian mixture model is compared with what is utilized in the design of wind turbines as given in the IEC 61400-1. The Gaussian mixture model is able to model the joint distribution of wind parameters well, where the estimated tail distributions of both the marginal distributions and conditional distribution have good accuracy, and it is a good candidate for extreme turbulence estimation.

1 Introduction

Wind turbulence is characterized by the turbulence kinetic energy, its dissipation rate, and the length scale. This is modeled using three-dimensional anisotropic spectra that captures the auto-correlation and cross-correlation of the spatio-temporal wind speed variation such as through the Mann model (Mann, 1994). Such models assume the wind turbulence is a Gaussian process, whereby several frequencies of wind velocity variations may occur resulting in different wind velocities distributed as

a function of time and space. Usually, the wind turbulence for wind turbine design is specified over a 10-minute time window and the stochastic process is assumed to be stationary. The occurrences of extreme turbulence can then be categorized based on its return period. In wind turbine design, the wind turbulence with a 50-year return period is used in ultimate limit state analysis (IEC, 2019).

Many uncertainties exist in the evaluation of the design loads of wind turbine components. The IEC 61400-1 standard lists several load cases of the relevance of ultimate limit state analysis, wherein the load cases under normal operation usually require a partial safety factor (PSF) of 1.35 applied to the characteristic loads. Such PSFs are determined by quantifying the uncertainties in the load evaluation (Sørensen and Toft, 2014) and the underlying distributions of the relevant inputs. An important load-case towards determining ultimate design loads on wind turbine structures is the Design Load Case (DLC) 1.3, in which the turbine is under normal operation under 50-year extreme wind turbulence. While relationships to evaluate the extreme turbulence level are provided in the IEC 61400-1, there has been much debate on its accuracy and quantification; with the edition-3 of the IEC 61400-1 specifying a lognormal distribution for turbulence and edition-4 specifying it as a Weibull distribution. Several studies (Dimitrov et al., 2017; Abdallah et al., 2016) have proposed different models for extreme wind turbulence based on site measurements and a large uncertainty can be seen in determining the long-term behavior of wind turbulence. Mathematically, an issue with the modelling of wind turbulence has been that the IEC 61400-1 standard and literature have mainly focused on the probability distribution of the standard deviation of the wind speed (σ_u) conditional on the mean of the longitudinal wind speed over a 10-minute time duration (u), whereas it is required that the joint distribution of σ_u and u is properly modeled.

A joint distribution model could be used for modelling multivariate random variables and generating random samples. Theoretical bivariate distributions are limited and not flexible enough. Monahan (2018) model the joint probability distribution of wind speeds at different locations using bivariate Rice distribution and bivariate Weibull distribution. The joint distribution of random variables could also be described by the univariate marginal distribution functions and a copula. A copula is a multivariate cumulative distribution function, where the marginal distribution follows uniform distribution on the interval [0,1]. Copulas are used for modelling the dependency among the random variables. Several families of copulas have been proposed in the literature, e.g., Gaussian copula (Nataf transformation (Xiao, 2014)) and Archimedean copulas (Bouyé et al., 2011). Using marginal distributions and copula to model the multivariate distributions is feasible, but the marginal distributions should be flexible enough to represent the wind inflow under varying environmental conditions, and the tail of the fitted distribution should be well representative of the actual inflow behavior. The copula structures should also be flexible enough to model different correlation structures. It is not clear as to which copula model (Abdallah, 2015) to choose to determine the joint distribution, given marginal distributions.

To model the extreme turbulence well, both the main body and the tail of the joint probability distribution of σ_u and u should be accurately represented. Gaussian mixture model (GMM) is broadly used for clustering tasks (Zhang et al., 2021). GMM is a flexible model which can also perform density estimation on multivariate data with different marginal distributions and correlation structures. It is widely applied to different fields of study, e.g., speech and audio processing (Reynolds and Rose, 1995), image classification (Permuter et al., 2003), density estimation of microarray data in bioinformatics (Steinhoff et al.,

2003), cancer classification (Prabakaran et al., 2019) and finance (Miyazaki et al., 2014). GMM is less commonly applied in wind energy compared to other domains, Chang et al. (2017) used GMM based neural network for short-term wind power forecast, Cui et al. (2018) used GMM for fitting the probability distribution of wind power ramping features, Zhang et al. (2019) used GMM for wind turbine power dispatching, Li et al. (2020) used GMM for electrical loads forecast, and Srbinovski et al. (2021) used GMM for modelling the site-specific wind turbine power curves. GMM has been rarely adopted for wind parameters modelling, Wahbah et al. (2018) used univariate GMM for wind speed probability density estimation, where the joint distribution of wind speed with other parameters was not investigated. Few published literature uses GMM for density estimation of wind inflow parameters and GMM has not been used for modelling the joint distribution of u and σ_u.

In this paper, GMM is used for modelling the joint distribution of wind parameters u and σ_u. GMM is firstly used for density estimation of a random sample from theoretical bivariate t distribution. Then it is used for modelling the wind parameters from both offshore and onshore sectors. GMM is benchmarked to the measurement data by comparing the marginal distributions and the conditional distributions. The wind parameter contour with a 50-year return period is also computed from GMM model with IFORM analysis (Winterstein et al., 1993). For the wind parameters from the offshore sector, Gaussian copula (Nataf transformation) and Gumbel copula are also compared.

2   Gaussian mixture model

GMM (McLachlan and Peel, 2000) is a mixture of several weighted Gaussian distributions and has been used for cluster analysis (Janouek et al., 2015) and density estimation (Steinhoff et al., 2003). GMM could be used for hard clustering and soft clustering of data. For hard clustering, each observation is assigned to the component returning the highest posterior probability, where each observation is assigned to exactly one cluster. Soft clustering, as opposed to hard clustering, assigns each observation to more than one cluster and each observation is assigned a responsibility (relative density). In terms of density estimation, the GMM is useful for multivariate distribution representations with multiple modes, but this does not prevent it from also being used for single mode distributions. GMM is a linear combination of multivariate Gaussian distribution components, where each component is defined by its mean and covariance. Even though a weighted sum of Gaussian random variables is a Gaussian random variable, a weighted Gaussian distribution is not necessarily Gaussian. When there are more than two components for GMM, it is multi-modal and is not Gaussian distributed. The probability distribution function (pdf) of a d-dimensional multivariate Gaussian is

$$\mathcal{N}\left(\mathbf{x}|\mu,\textstyle\sum\right) = \frac{1}{\sqrt{|\sum|(2\pi)^d}} \exp\left(-\frac{1}{2}(\mathbf{x}-\mu)\textstyle\sum^{-1}(\mathbf{x}-\mu)^{\mathrm{T}}\right) \tag{1}$$

where μ is the 1-by-d mean vectors, and $\sum$ is the d-by-d covariance matrix. The pdf of GMM is

$$p(\mathbf{x}) = \sum_{j=1}^{k} \pi_j \mathcal{N}\left(\mathbf{x}|\mu_j, \textstyle\sum_j\right) \tag{2}$$

where k is the number of components, which is a hyper parameter, and π_j is the component coefficient (weight) and follows

$$\sum_{j=1}^{k} \pi_j = 1 \quad 0 \leq \pi_j \leq 1 \tag{3}$$

Some information criteria are proposed in the literature (Akaike, 1998; Schwarz, 1978) to determine k, where k is selected as a balance of overfitting and underfitting. Nevertheless, when the sample size is too large, the criteria are not effective and further research is required. To use GMM for density estimation and also for random sample generation, the model parameters $\{\pi_j, \mu_j, \Sigma_j, j = 1, 2, ..., k\}$ should be estimated from the data sample $\{\mathbf{x}_n, n = 1, 2, ..., N\}$, where N is the sample size. The initial model parameters are calculated from the clusters evaluated by the k-means clustering algorithm (Arthur and Vassilvitskii, 2006), and optimized by the Expectation-Maximization (EM) algorithm (McLachlan et al., 2019) as follows:

1. Assign the N observations to the k clusters using the k-means clustering algorithm. Compute μ_j, Σ_j and π_j from the observations within each cluster.

   k-means clustering assigns N observations to k clusters, which are defined by the centroids. Each data point x_n with the closest centroid is assigned to the corresponding cluster. The centroids are recalculated and the data points are reassigned until the clusters do not change or the maximum iteration number is met. This is a hard clustering, and within each component, the μ_j and Σ_j are calculated, and the π_j is calculated as the number of data points in the current cluster divided by N.

2. Expectation-Maximization (EM) algorithm

   The model parameters $\{\pi_j, \mu_j, \Sigma_j, j = 1, 2, ..., k\}$ are found by an iterative EM algorithm (Dempster et al., 1977) to have a maximum likelihood estimation.

   (a) E step

   Evaluate the responsibilities using the current model parameters. The responsibility $\gamma_j(\mathbf{x}_n)$ is the probability that component j takes for explaining the observation $\mathbf{x}_n$, which is calculated as:

   $$\gamma_j(\mathbf{x}_n) = \frac{\pi_j \mathcal{N}\left(\mathbf{x}_n | \mu_j, \Sigma_j\right)}{\sum_{i=1}^{k} \pi_i \mathcal{N}\left(\mathbf{x}_n | \mu_i, \Sigma_i\right)} \tag{4}$$

   (b) M step

   Update the model parameters using the responsibilities from E step. The mean for component j is calculated as:

   $$\mu_j = \frac{\sum_{n=1}^{N} \gamma_j(\mathbf{x}_n)\mathbf{x}_n}{\sum_{n=1}^{N} \gamma_j(\mathbf{x}_n)} \tag{5}$$

   The covariance for component j is calculated as:

   $$\Sigma_j = \frac{\sum_{n=1}^{N} \gamma_j(\mathbf{x}_n)(\mathbf{x}_n - \mu_j)(\mathbf{x}_n - \mu_j)^T}{\sum_{n=1}^{N} \gamma_j(\mathbf{x}_n)} \tag{6}$$

and the j component coefficient is calculated as:

$$\pi_j = \frac{1}{N} \sum_{n=1}^{N} \gamma_j(\mathbf{x}_n) \tag{7}$$

120   3. Repeat step 2 until the model parameters converge or the maximum number of iterations is met.

3   Results

GMM is proposed to model the joint distribution of u and σ_u, where the estimation error is small at both the main body pdf and the tail distribution. To verify the use of GMM, it is firstly used to recover the multivariate t distribution from a t distribution random sample. The flexibility of GMM (especially for modelling non-Gaussian joint distribution) and the demonstration of

125   the procedure of using GMM for density estimation is detailed. To sample from the fitted joint-distribution is very important as many reliability analysis and uncertainty quantification applications require random samples as inputs. The random samples from GMM are compared with the random sample from the t distribution and wind parameters. To compute the number of components k, it is increased from 1 until the estimated density function converges.

Using copulas to develop non-Gaussian joint distributions of the u and σ_u is initially attempted. A joint probability distribu-

130   tion of the u and σ_u is then modelled by GMM. For estimating the extreme turbulence (wind parameter contour with 50-year return period), the accuracy of tail distribution is important. The probability of exceedance of σ_u conditional on u from GMM is thus compared with the measurement data. To further examine the flexibility of GMM, the wind measurement data from both the offshore and onshore sectors are investigated and the 50-year wind parameter contour are compared.

3.1   Multivariate t distribution

135   The pdf of the d-dimensional multivariate Student's t distribution is

$$f\left(\mathbf{x}, \Sigma, v\right) = \frac{1}{|\Sigma|^{1/2}} \frac{1}{\sqrt{(v\pi)^d}} \frac{\Gamma\left((v+d)/2\right)}{\Gamma(v/2)} \left(1 + \frac{\mathbf{x}'\Sigma^{-1}\mathbf{x}}{v}\right) \tag{8}$$

where Σ is a correlation matrix with a correlation coefficient 0.6, and $v = 5$ is the degrees of freedom. The multivariate Student's t distribution generalizes the univariate Student's t distribution, and its marginal distributions all have univariate Student's t distribution. The marginal distributions of multivariate Student's t distribution have fatter tails than the normal

140   distribution. A random sample with size 10^5 is generated from the bivariate t distribution, and GMM is used to fit the bivariate t distribution.

The estimated density function converges when the number of components $k = 4$, and therefore, the k-means clustering algorithm is used to cluster the data points into $k = 4$ components. The mean, covariance, and the component coefficient (sample size at each component divided by the total sample size) calculated from each component are taken as initial parameters

145   for GMM, which are shown in Table. 1. The four clusters are plotted in Fig. 1, where the means are plotted in circles.

Following the procedure of EM algorithm (see section 2), the model parameters are estimated, which are shown in Table 2. Fig. 2 shows the random sample from t distribution and GMM, and Fig. 3 shows the corresponding contour plots. The random

Table 1. Initial GMM parameters

Component number (i)	1	2	3	4
μ_i	$\begin{bmatrix} -1.972 & -2.037 \end{bmatrix}$	$\begin{bmatrix} 1.978 & 1.966 \end{bmatrix}$	$\begin{bmatrix} -0.552 & -0.522 \end{bmatrix}$	$\begin{bmatrix} 0.521 & 0.511 \end{bmatrix}$
Σ_i	$\begin{bmatrix} 1.242 & 0.067 \\ 0.067 & 1.273 \end{bmatrix}$	$\begin{bmatrix} 1.237 & 0.128 \\ 0.128 & 1.128 \end{bmatrix}$	$\begin{bmatrix} 0.396 & -0.155 \\ -0.155 & 0.396 \end{bmatrix}$	$\begin{bmatrix} 0.384 & -0.155 \\ -0.155 & 0.396 \end{bmatrix}$
π_i	0.107	0.111	0.388	0.395
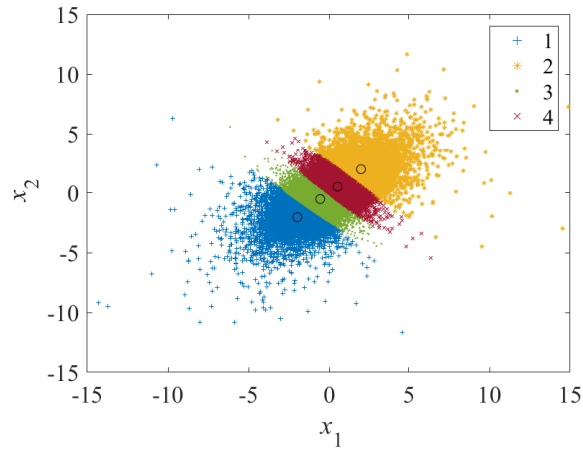
Figure 1. k-means clustering of t distribution sample

sample from GMM has a similar correlation structure with the theoretical t distribution. For probability densities higher than 10^{-5}, GMM agrees well with the theoretical t distribution; for lower densities, there is some deviation, which is due to the
150   small sample size and sample variation.

Table 2. Final GMM parameters

Component number (i)	1		2		3		4	
μ_i	$\begin{bmatrix} -1.80 & -0.736 \end{bmatrix}$		$\begin{bmatrix} 0.016 & 0.001 \end{bmatrix}$		$\begin{bmatrix} -0.011 & -0.004 \end{bmatrix}$		$\begin{bmatrix} 0.014 & 0.015 \end{bmatrix}$	
Σ_i	$\begin{bmatrix} 24.655 & 11.076 \\ 11.076 & 21.447 \end{bmatrix}$		$\begin{bmatrix} 4.794 & 2.937 \\ 2.937 & 4.900 \end{bmatrix}$		$\begin{bmatrix} 1.505 & 0.891 \\ 0.891 & 1.508 \end{bmatrix}$		$\begin{bmatrix} 0.586 & 0.354 \\ 0.354 & 0.580 \end{bmatrix}$	
π_i	0.004		0.119		0.504		0.373	
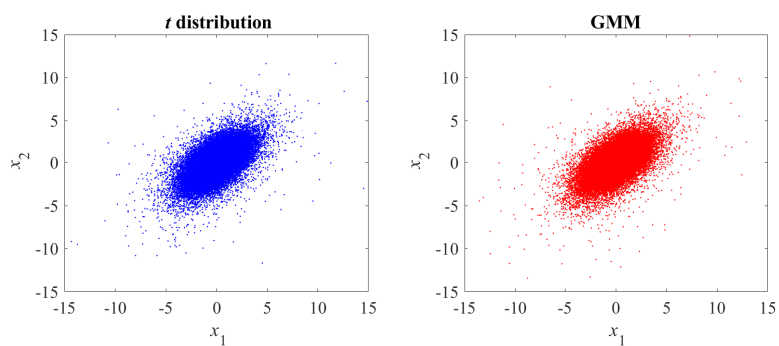
Figure 2. Random sample from t distribution and GMM
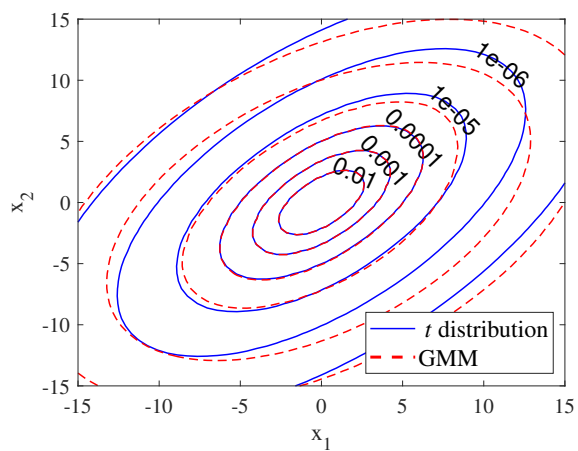
Figure 3. Contour plot of t distribution and GMM

3.2 Wind measurements

The wind measurements from the Høvsøre Test Centre for Large Wind Turbines in western Denmark (Dimitrov et al., 2017; Hannesdóttir et al., 2019) are used in this study. The 10-min high-frequency time series of three-dimensional wind velocities at a height of 100 meters is selected. The period of measurements is from 1 January, 2005 to 1 January, 2020, i.e. 15 years of

155 measurement data (Hannesdóttir et al., 2019). u and σ_u, which is linearly detrended, are calculated from 10-min time series. The wind parameters from the offshore sector (225° to 315°) and onshore sectors (150° to 180° and 45° to 135°) are studied here. Outliers and potentially missing data elements are omitted. The sensors on the Høvsøre mast have been replaced regularly and calibrated, the data used in this paper is calibrated data (Peña et al., 2016). The sample size is about 2.43×10^5 for the offshore sector, 4.09×10^4 for the onshore sector (150° to 180°), and 1.41×10^5 for the onshore sector (45° to 135°). The wind

160 speed variation is considered to be stationary, and non-stationary wind conditions are not included in this study.
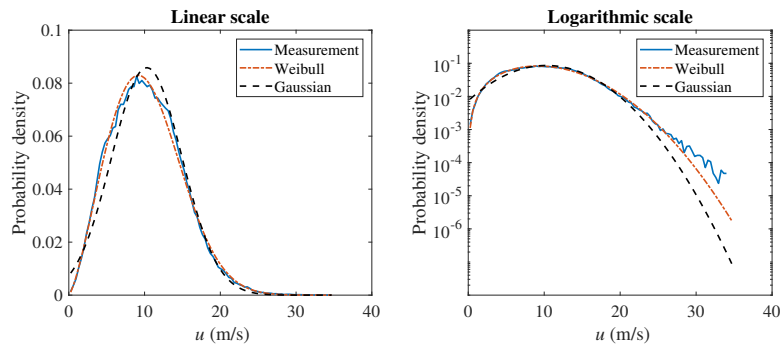
Figure 4. Marginal distribution of u with Weibull fitting
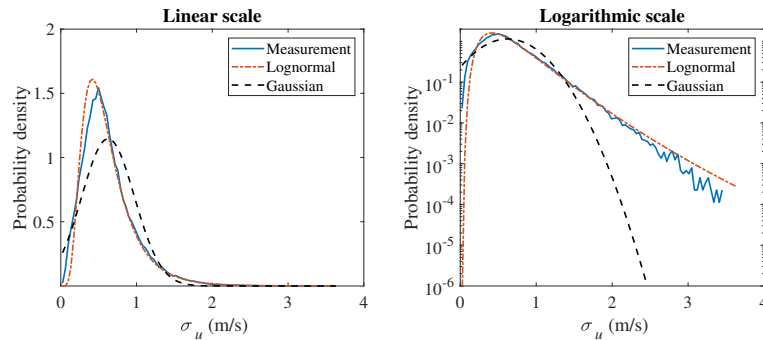
Figure 5. Marginal distribution of σ_u with lognormal fitting

The marginal distributions to be used are to be defined and the correlation between the variables is modelled by the copula structure. Here, a Weibull distribution is used for modelling the marginal distribution of u, where the scale parameter is 11.61 and the shape parameter is 2.35. The plots are shown in Fig. 4. The lognormal distribution is used for modelling the marginal

distribution of σ_u, where the mean and standard deviation of logarithmic values are -0.61 and 0.52. The plots are shown in Fig. 5. Both the linear and logarithmic scales are plotted, where the main body pdf and tail distribution could be compared. It can be seen that Weibull and lognormal distributions are good fits for the u and σ_u respectively. The univariate Gaussian distribution is also used here to fit the distribution of u and σ_u, but it is not a proper fit, which also indicates that the multivariate Gaussian distribution is not a good candidate for modelling the joint distribution of the wind parameters. The Nataf transformation (Xiao, 2014) and Gumbel copula are used here to model the joint distribution of u and σ_u and generate random samples. The generated random sample is shown in Fig. 6, where the left figure is the scatter plot of the measurement data, the middle figure is the Nataf transformation generated sample, and the right figure is the Gumbel copula generated sample. The Nataf transformation and Gumbel copula generated samples have the same sample size as the measurement data. They have the same fitted marginal distributions, but different copula structures, as is demonstrated in Fig. 6.
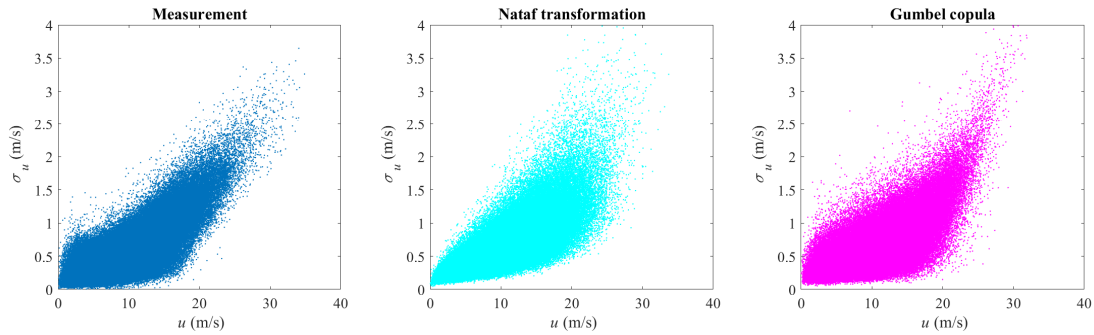
Figure 6. Nataf transformation and Gumbel copula random samples for offshore sector

The different copula structures lead to different conditional distributions. The Nataf transformation and Gumbel copula estimated probability of exceedance of σ_u conditional on u are shown in Fig. 7 and Fig. 8 respectively. Only the distributions $u \geq 16 \text{ ms}^{-1}$ are plotted as they are close to the tail and affect the 50-year turbulence estimation most. As is seen in Fig. 7, the probabilities of exceedance of σ_u conditional on u deviate from the measurement data significantly. Using a Gumbel copula as is shown in Fig. 8, even though there is a reasonable agreement when u ranges from 16 ms^{-1} to 20 ms^{-1}, a larger discrepancy arises for higher mean wind speeds. The differences in the conditional distribution between the copula-estimated and measurement data indicate that using copula could lead to a biased 50-year turbulence estimation and large model uncertainty for DLC 1.3 simulations.

Even though other copula structures are available, they are not flexible enough to represent the joint distribution of u and σ_u from different measurement sites or even the same site for different wind direction sectors. The correct copula to use to generate the joint distribution of u and σ_u for tail estimation requires further research. However, instead of fitting the joint distribution using copula methods, a multivariate distribution is another option. To perform density estimation on univariate random variables, many theoretical probability distributions are available, e.g., normal, Weibull, lognormal, Rayleigh distribution, and the methods in (Zhang et al., 2020; Low, 2013), etc. On the other hand, fewer probability distributions are available for
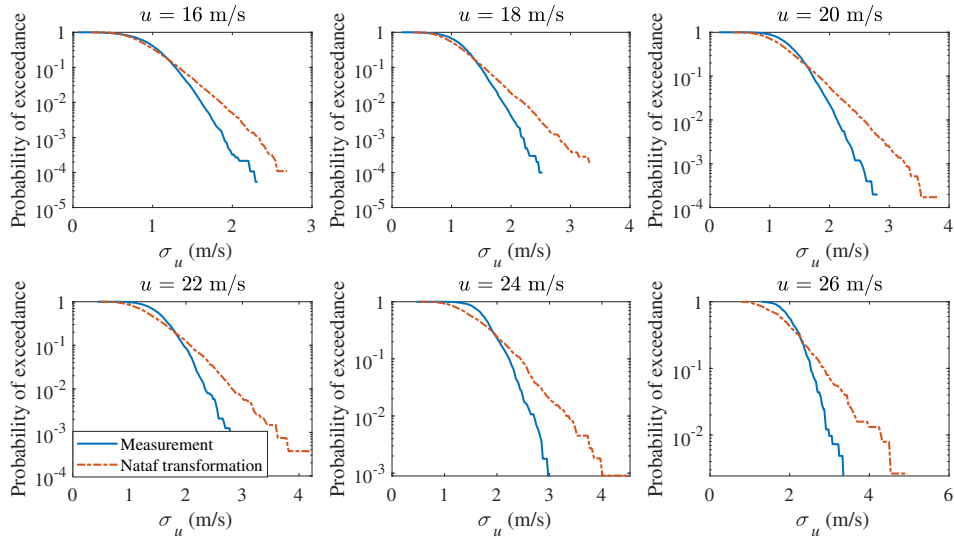
Figure 7. Nataf transformation probability of exceedance of σ_u conditional on u
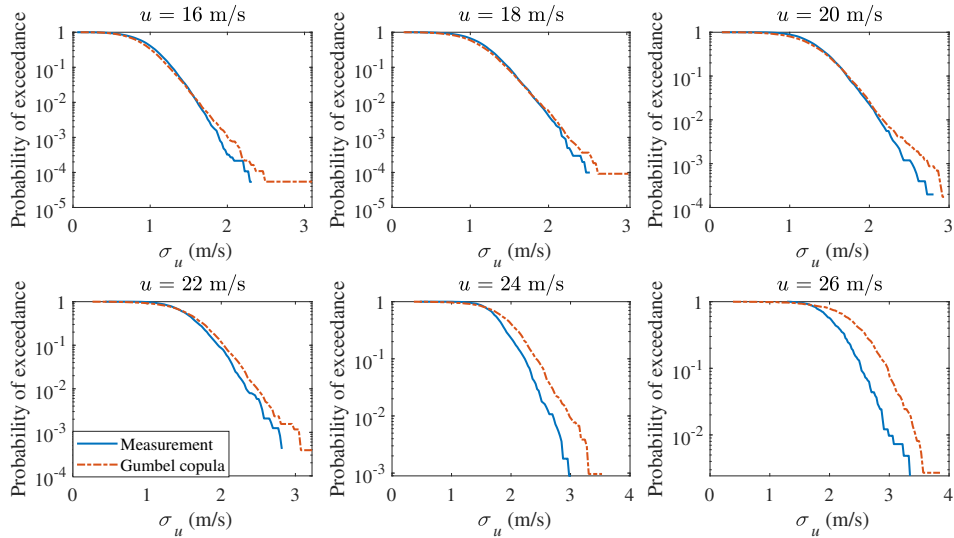
Figure 8. Gumbel copula probability of exceedance of σ_u conditional on u

multivariate density estimations. This creates a similar limitation of copula models, i.e., theoretical multivariate distributions are limited and not flexible enough to model the u and σ_u measurements that possess different correlation structures. GMM on the other hand is quite flexible since a number of Gaussian distributions with corresponding weights could be used to estimate the probability densities for multivariate variables and generate correlated samples.

3.3 GMM based estimation of wind parameters for the offshore sector

It is important to model the joint distribution of wind parameters, which could be used for uncertainty quantification, structural optimization, and reliability analysis of wind turbines. The joint distribution should have a small estimation error for a realistic 50-year turbulence estimation. For the copula examples in section 3.2, the marginal distributions are estimated well, but not the correlation structure, which leads to inaccuracies in the conditional distribution. Using GMM does not have the same limitation, as a good joint distribution estimation will estimate both marginal distributions and correlation structures with small estimation errors.
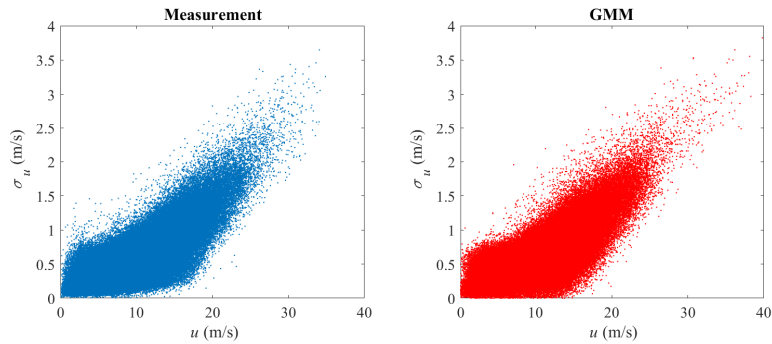
Figure 9. Measurement data and GMM random sample for offshore sector

GMM is adopted here to model the joint distribution of u and σ_u. The measurement data and GMM random samples are shown in Fig. 9, where the correlation structure of the measurement data is well captured. The marginal distribution of u is shown in Fig. 10 and the marginal distribution of σ_u is shown in Fig. 11. Compared to Figs. 4 and 5, the marginal distributions from GMM has smaller difference with the measurement data at both the main body pdf and the tails. The univariate Gaussian distribution is not a good fit for either of the marginal distribution, but GMM is a good fit as its marginal distribution is a linear combination of univariate Gaussian distributions (not necessarily Gaussian distribution), which is more flexible compared to Gaussian distribution. For marginal distribution estimation, which theoretical distribution to choose remains a problem, especially when the sample size is small and the tail might exhibit different shapes. GMM does not have the trouble of selecting distributions for marginal distribution estimation.
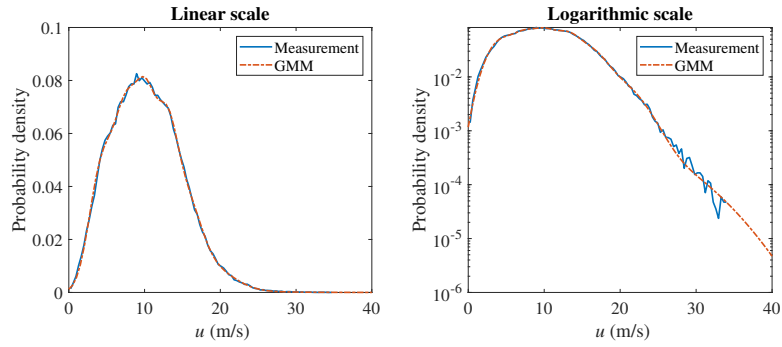
Figure 10. Marginal distribution of u for offshore sector
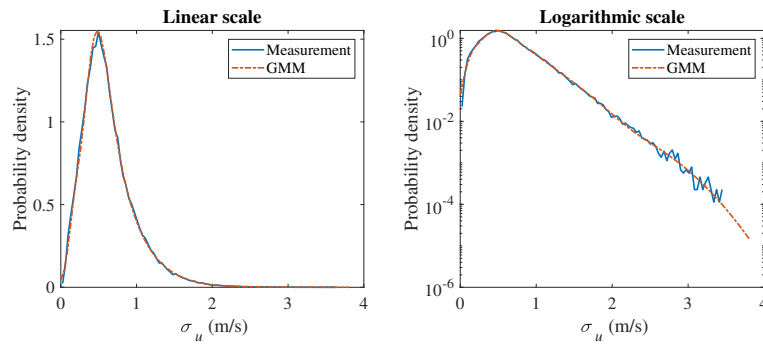
Figure 11. Marginal distribution of σ_u for offshore sector

The probability distribution of σ_u conditional on u is plotted in Fig. 12. The probability of exceedance of σ_u conditional on u is plotted in Fig. 13. Both the main body pdf and the probability of exceedance from GMM agree quite well with the measurement data, for the bins when $u = 26\ \mathrm{m\,s^{-1}}$, the tail of the measurement data is not accurate due to the small sample size (412).
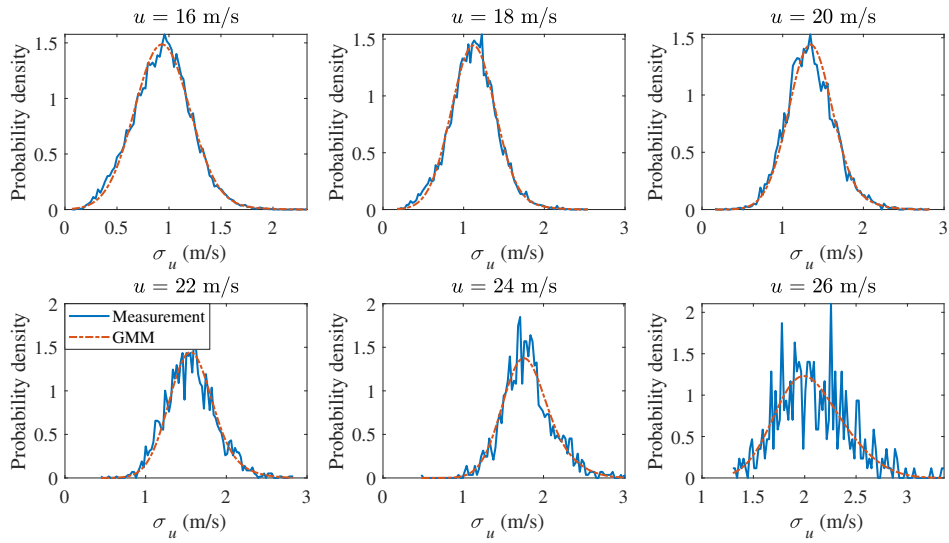
Figure 12. GMM probability distribution of σ_u conditional on u for offshore sector
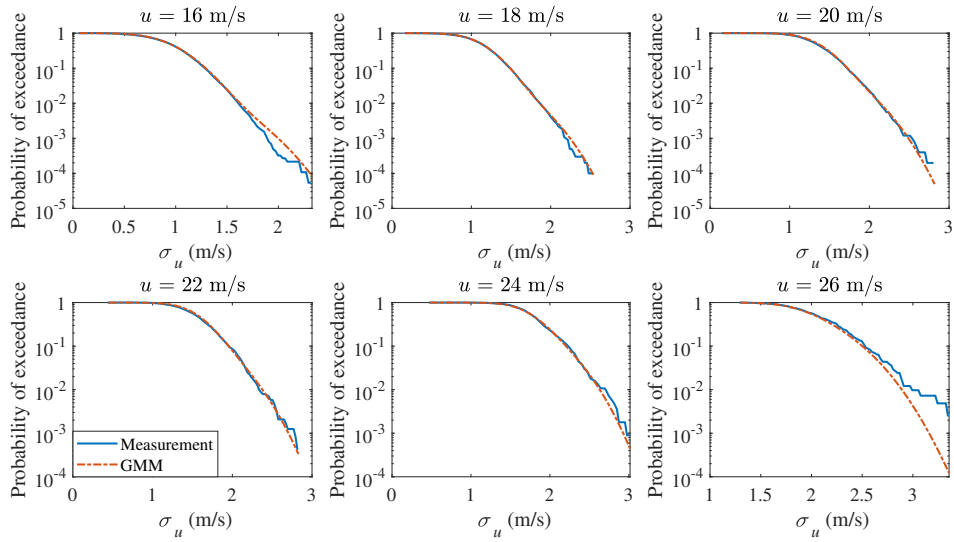
Figure 13. GMM probability of exceedance of σ_u conditional on u for offshore sector

The 10-min turbulence level (wind parameter contours) associated with a return period of 50 years as provided in the IEC 61400-1 and as computed by GMM are shown in Fig. 14. The contour labelled IEC (blue '+') uses a reference turbulence intensity $I_{ref} = 0.12$ (corresponding to wind turbine class C) as input to perform IFORM analysis (Winterstein et al., 1993; IEC, 2005), where u is modeled by Weibull distribution and the probability distribution of σ_u conditional on u is modeled by lognormal distribution (IEC, 2005). The IEC (data) (green 'x') is the same as the IEC (blue '+') except that $I_{ref} = 0.057$, which is calculated as the expected value of turbulence intensity at a mean wind speed of 15 ms^{-1} from the measurement data (IEC, 2005). The contour labelled IEC (data) has lower values than the contour labelled IEC, since I_{ref} is smaller (0.057 vs 0.12). The 50-year contour estimated using GMM with IFORM analysis (Winterstein et al., 1993) is realistic as it has a similar shape to the scatter plot of the measurement data and bounds the data points. The marginal distributions agree well with the measurement data (as are shown in Figs. 10 and 11), the conditional distributions are validated in Figs. 12 and 13. The IEC contour happens to be aligned with GMM, but the IEC 61400-1 does not prescribe a joint probability distribution or the marginal distribution for σ_u. As the I_{ref} used is much larger than obtained through the measurement data (0.12 vs 0.057), it could be inferred that the use of a lognormal distribution conditional on the mean wind speed or the empirical formulas in (IEC, 2005) might not be accurate. The fourth edition of the IEC 61400-1 (IEC, 2019) does not increase the accuracy with the Weibull distribution for turbulence conditional on the mean wind speed, as the 50-year turbulence level is still unchanged.
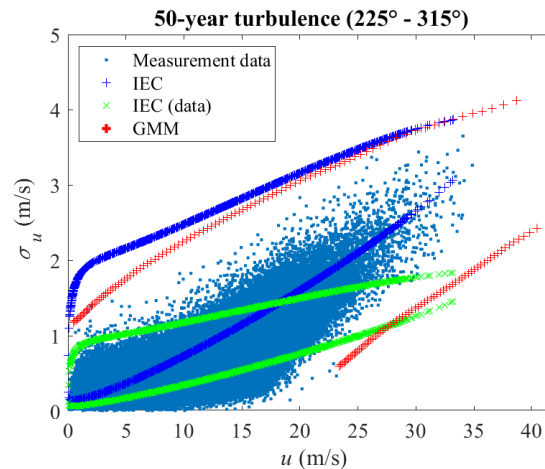
Figure 14. GMM and IEC 50-year turbulence estimation for offshore sector

3.4 GMM based estimation of wind parameters for the onshore sectors

It is worth investigating the applicability of GMM to other wind direction sectors, where the wind parameters have different correlation structures due to different terrains. The u and σ_u in the onshore section (150° to 180°) are modelled using GMM. The measurement data and a random sample from GMM are shown in Fig. 15, where the correlation structure is different from the offshore sector in Fig. 9. The marginal distribution of u is shown in Fig. 16 and the marginal distribution of σ_u is shown in Fig. 17. Negligible differences could be seen from the comparison of the main body pdfs and the tails. The probability distribution of σ_u conditional on u is plotted in Fig. 18. The probability of exceedance of σ_u conditional on u is plotted in Fig. 19. Note that the sample size is smaller than the offshore sector (4.09×10^4 vs 2.43×10^5), so the tail distribution of the onshore measurement data has lesser accuracy as compared to the offshore sector, but still performs better than using the method of copulas. The 50-year turbulence contour is shown in Fig. 20, where the left figure shows the 50-year turbulence estimated from the measurement data from the sector with direction from 150° to 180°, and the right figure is from the sector with direction from 45° to 135°. A slightly larger 50-year contour is estimated from the 45° to 135° sector. Figures 18 - 20 show that GMM is indeed flexible and can be used to model u and σ_u for different wind conditions, albeit for flat terrains.
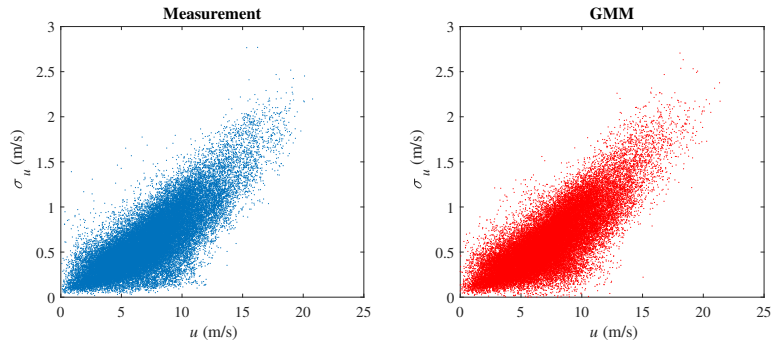
Figure 15. Measurement data and GMM random sample for onshore sector

Note that the estimated density function converges when $k = 8$ for all the joint distribution estimations of wind parameters using GMM. More components are needed compared to the theoretical t distribution (8 vs 4) as the correlation structure between the u and σ_u is more complex.
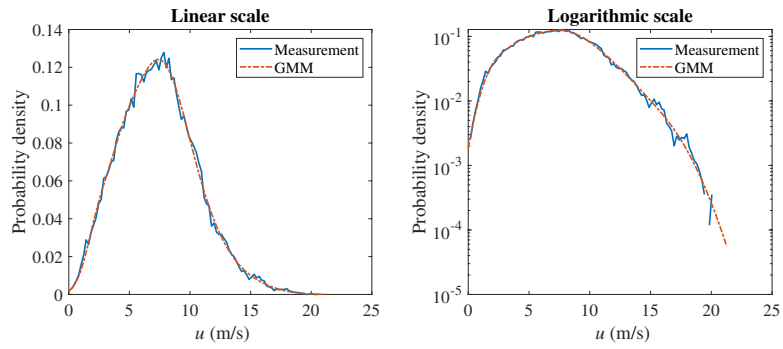
Figure 16. GMM marginal distribution of u for onshore sector
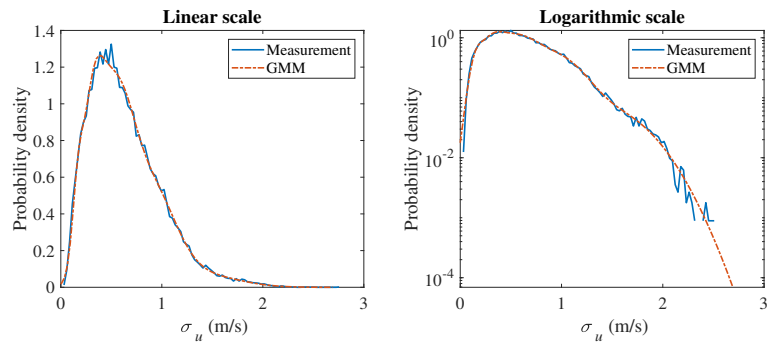
Figure 17. GMM marginal distribution of σ_u for onshore sector
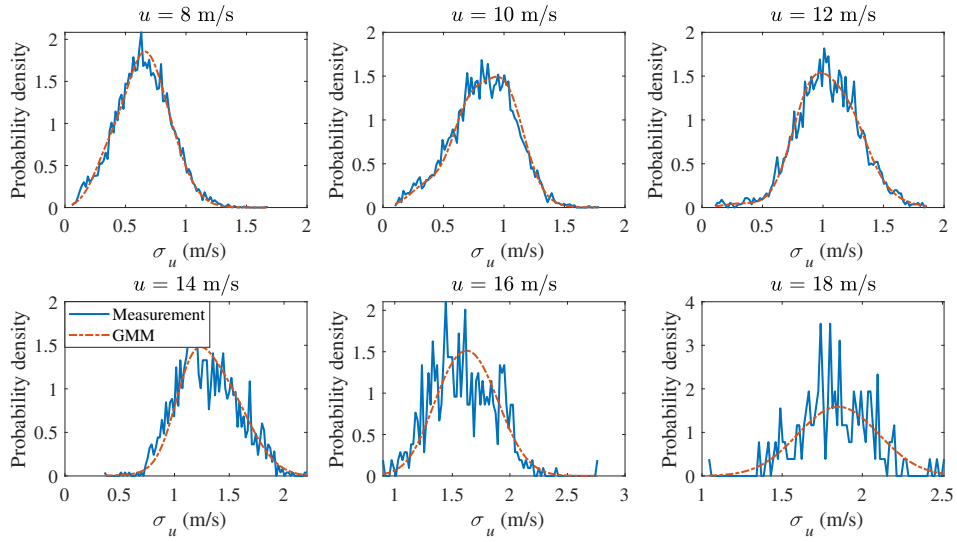
Figure 18. GMM probability distribution of σ_u conditional on u for onshore sector
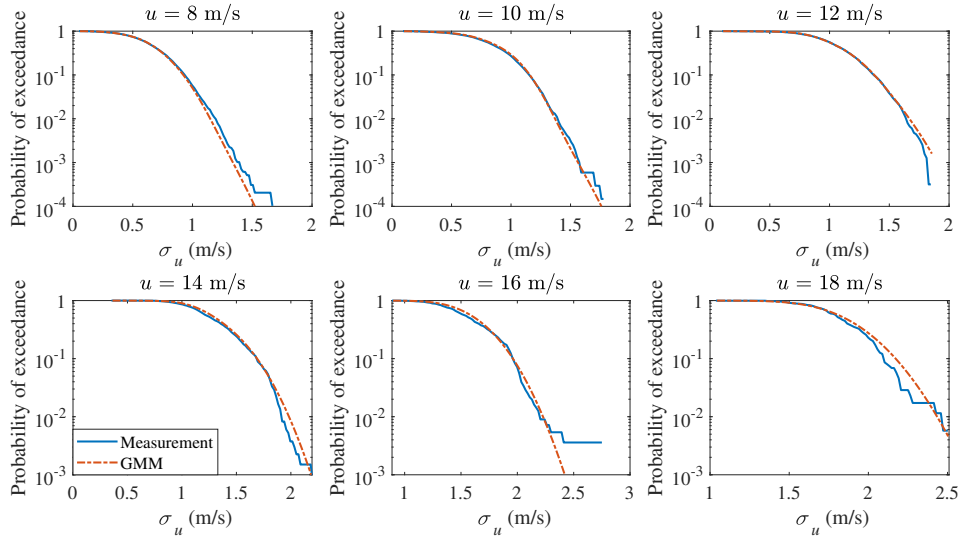
Figure 19. GMM probability of exceedance of σ_u conditional on u for onshore sector
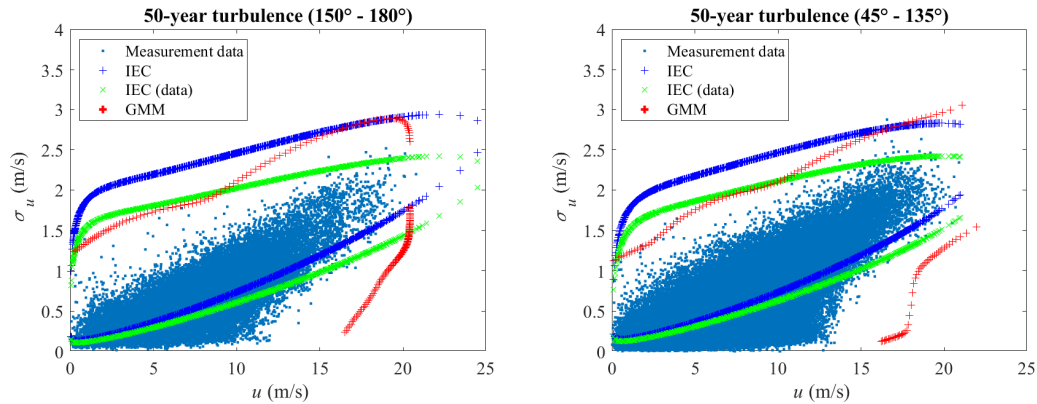
Figure 20. GMM and IEC 50-year turbulence estimation for two onshore sectors

4 Conclusions

GMM is proposed to model the joint distribution of wind parameters, i.e., u and σ_u, and it is readily implementable and provides realistic 50-year turbulence levels. This model has been validated using multi-year high frequency wind velocity measurements at one site for offshore climate and for flat land terrains. Copula-based joint probability models were not found to have the flexibility to accurately model the tails of σ_u conditional on u.

A procedure using GMM that properly captures the joint distribution of wind parameters is proposed. Both the marginal distributions of u and σ_u, and the distribution of σ_u conditional on u were shown to reflect the multi-year wind measurements. This model allows a good estimation of the 50-year turbulence (validated by the marginal and conditional distributions), which serves as an input to wind turbine design load cases. The procedure of GMM is demonstrated by fitting the theoretical multivariate t distribution. GMM is then used to estimate the probability distribution of offshore wind parameters and two-sector onshore wind parameters. There is a good agreement between GMM estimated probability distribution and the measurement data. The 50-year wind parameter contour is estimated from GMM and compared with the corresponding values based on the IEC 61400-1. The applicability to different sectors of the wind measurement data demonstrates its flexibility and shows its potential for modelling the joint distribution of wind parameters. Compared to copula methods, it has less estimation error for the estimated marginal distributions and conditional distributions.

The determination of the optimal number of components for GMM requires further research. In this paper, four components was found to be required to sufficiently model the theoretical t distribution and eight components were required to model the wind parameters for both offshore and onshore sectors of the chosen site. As more components are used, the pdf of GMM will converge to the target distribution, but will require more computational efforts (several minutes on a standard laptop computer). Another limitation for GMM is that it might not extrapolate well for certain correlation structures, especially if the sample size is small, even though the model is quite flexible.

Author contributions. XZ developed the methodology with contributions from AN, XZ implemented the scientific methods and validated the results, XZ wrote the original draft of the paper. AN conceived the original idea, supervised the scientific work, reviewed and edited the paper.

Competing interests. The authors declare that they have no competing interest.

Acknowledgements. This work has received funding from the Danish Energy Technology Development and Demonstration Program, EUDP, under the project ProbWind, with grant agreement 64019-0587.

References

Abdallah, I.: Assessment of extreme design loads for modern wind turbines using the probabilistic approach, 2015.

Abdallah, I., Natarajan, A., and Sørensen, J. D.: Influence of the control system on wind turbine loads during power production in extreme turbulence: Structural reliability, Renewable Energy, 87, 464–477, https://doi.org/10.1016/j.renene.2015.10.044, 2016.

Akaike, H.: Information theory and an extension of the maximum likelihood principle, in: Selected papers of hirotugu akaike, pp. 199–213, Springer, 1998.

Arthur, D. and Vassilvitskii, S.: k-means++: The advantages of careful seeding, Tech. rep., Stanford, 2006.

Bouyé, E., Durrleman, V., Nikeghbali, A., Riboulet, G., and Roncalli, T.: Copulas for finance - a reading guide and some applications, SSRN Electronic Journal, https://doi.org/10.2139/ssrn.1032533, 2011.

Chang, G. W., Lu, H. J., Wang, P. K., Chang, Y. R., and Lee, Y. D.: Gaussian mixture model-based neural network for short-term wind power forecast, International Transactions on Electrical Energy Systems, 27, e2320, https://doi.org/10.1002/etep.2320, 2017.

Cui, M., Feng, C., Wang, Z., and Zhang, J.: Statistical representation of wind power ramps using a generalized Gaussian mixture model, Ieee Transactions on Sustainable Energy, 9, 261–272, https://doi.org/10.1109/TSTE.2017.2727321, 2018.

Dempster, A. P., Laird, N. M., and Rubin, D. B.: Maximum likelihood from incomplete data via the EM algorithm, Journal of the Royal Statistical Society. Series B (Methodological), 39, 1–38, http://www.jstor.org/stable/2984875, 1977.

Dimitrov, N. K., Natarajan, A., and Mann, J.: Effects of normal and extreme turbulence spectral parameters on wind turbine loads, Renewable Energy, 101, 1180–1193, https://doi.org/10.1016/j.renene.2016.10.001, 2017.

Hannesdóttir, Á., Kelly, M., and Dimitrov, N.: Extreme wind fluctuations: Joint statistics, extreme turbulence, and impact on wind turbine loads, Wind Energy Science, 4, 325–342, https://doi.org/10.5194/wes-4-325-2019, 2019.

IEC: International Standard IEC61400-1: Wind Turbines - Part 1: Design Guidelines, 2005.

IEC: International Standard IEC61400-1: Wind Turbines - Part 1: Design Guidelines, 2019.

Janouek, J., Gajdo, P., Radecky, M., and Snasel, V.: Gaussian mixture model cluster forest, Proceedings - 2015 Ieee 14th International Conference on Machine Learning and Applications, Icmla 2015, pp. 1019–1023, https://doi.org/10.1109/ICMLA.2015.12, 2015.

Li, T., Wang, Y., and Zhang, N.: Combining probability density forecasts for power electrical loads, Ieee Transactions on Smart Grid, 11, 1679–1690, https://doi.org/10.1109/TSG.2019.2942024, 2020.

Low, Y. M.: A new distribution for fitting four moments and its applications to reliability analysis, Structural Safety, 42, 12–25, https://doi.org/10.1016/j.strusafe.2013.01.007, 2013.

Mann, J.: The spatial structure of neutral atmospheric surface-layer turbulence, Journal of Fluid Mechanics, 273, 141–168, https://doi.org/10.1017/S0022112094001886, 1994.

McLachlan, G. J. and Peel, D.: Finite mixture models, Wiley, 2000.

McLachlan, G. J., Lee, S. X., and Rathnayake, S. I.: Finite Mixture Models, p. 26, 2019.

Miyazaki, B., Izumi, K., Toriumi, F., and Takahashi, R.: Change detection of orders in stock markets using a Gaussian mixture model, Intelligent Systems in Accounting, Finance and Management, 21, 169–191, https://doi.org/10.1002/isaf.1356, 2014.

Monahan, A. H.: Idealized models of the joint probability distribution of wind speeds, Nonlinear Processes in Geophysics, 25, 335–353, https://doi.org/10.5194/npg-25-335-2018, 2018.

Peña, A., Floors, R., Sathe, A., Gryning, S.-E., Wagner, R., Courtney, M. S., Larsén, X., Hahmann, A. N., Hasager, C. B., et al.: Ten years of boundary-layer and wind-power meteorology at Høvsøre, Denmark, Boundary-Layer Meteorology, 158, 1–26, 2016.

Permuter, H., Francos, J., and Jermyn, I. H.: Gaussian mixture models of texture and colour for image database retrieval, Icassp, Ieee International Conference on Acoustics, Speech and Signal Processing - Proceedings, 3, 569–572, 2003.

Prabakaran, I., Wu, Z., Lee, C., Tong, B., Steeman, S., Koo, G., Zhang, P. J., and Guvakova, M. A.: Gaussian mixture models for probabilistic classification of breast cancer, Cancer Research, 79, 3492–3502, https://doi.org/10.1158/0008-5472.CAN-19-0573, 2019.

Reynolds, D. and Rose, R.: Robust text-independent speaker identification using Gaussian mixture speaker models, Ieee Transactions on Speech and Audio Processing, 3, 72–83, https://doi.org/10.1109/89.365379, 1995.

Schwarz, G.: Estimating the dimension of a model, The annals of statistics, pp. 461–464, 1978.

Srbinovski, B., Temko, A., Leahy, P., Pakrashi, V., and Popovici, E.: Gaussian mixture models for site-specific wind turbine power curves, Proceedings of the Institution of Mechanical Engineers, Part A: Journal of Power and Energy, 235, 494–505, https://doi.org/10.1177/0957650920931729, 2021.

Steinhoff, C., Müller, T., Nuber, U. A., and Vingron, M.: Gaussian mixture density estimation applied to microarray data, Lecture Notes in Computer Science (including Subseries Lecture Notes in Artificial Intelligence and Lecture Notes in Bioinformatics), 2810, 418–429, https://doi.org/10.1007/978-3-540-45231-7_39, 2003.

Sørensen, J. D. and Toft, H. S.: Safety factors–IEC 61400-4-background document, 2014.

Wahbah, M., Alhussein, O., El-Fouly, T. H., Zahawi, B., and Muhaidat, S.: Evaluation of parametric statistical models for wind speed probability density estimation, 2018 Ieee Electrical Power and Energy Conference, Epec 2018, p. 8598283, https://doi.org/10.1109/EPEC.2018.8598283, 2018.

Winterstein, S. R., Ude, T. C., Cornell, C. A., Bjerager, P., and Haver, S.: Environmental parameters for extreme response: Inverse FORM with omission factors, Proceedings of the ICOSSAR-93, Innsbruck, Austria, pp. 551–557, 1993.

Xiao, Q.: Evaluating correlation coefficient for Nataf transformation, Probabilistic Engineering Mechanics, 37, 1–6, https://doi.org/10.1016/j.probengmech.2014.03.010, 2014.

Zhang, J., Yan, J., Infield, D., Liu, Y., and sang Lien, F.: Short-term forecasting and uncertainty analysis of wind turbine power based on long short-term memory network and Gaussian Mixture Model, Applied Energy, 241, 229–244, https://doi.org/10.1016/j.apenergy.2019.03.044, 2019.

Zhang, X., Low, Y. M., and Koh, C. G.: Maximum entropy distribution with fractional moments for reliability analysis, Structural Safety, 83, 101 904, https://doi.org/10.1016/j.strusafe.2019.101904, 2020.

Zhang, Y., Li, M., Wang, S., Dai, S., Luo, L., Zhu, E., Xu, H., Zhu, X., Yao, C., and Zhou, H.: Gaussian mixture model clustering with incomplete data, ACM Transactions on Multimedia Computing, Communications, and Applications (TOMM), 17, 1–14, 2021.